Alternative Method for Determining Surface Energy by Utilizing Polymer Thin Film Dewetting

ARTICLE *in* LANGMUIR · JANUARY 2003

Impact Factor: 4.46 · DOI: 10.1021/la026489m

2 AUTHORS, INCLUDING:

Bi-min Zhang Newby
University of Akron
49 PUBLICATIONS **887** CITATIONS

SEE PROFILE

Alternative Method for Determining Surface Energy by Utilizing Polymer Thin Film Dewetting

Sung-Hwan Choi and Bi-min Zhang Newby*

Department of Chemical Engineering, The University of Akron, Akron, Ohio 44325-3906

Received August 28, 2002. In Final Form: November 20, 2002

Contact angle and contact mechanics, the most common estimating methods for surface energy, exhibit intrinsic drawbacks when determining surface energy or surface energy variation of micron-scaled areas. In this study, the dewetting of a polymer thin film was explored as a means for surface energy determination. In particular, two empirical plots were generated through modification of silicon wafers with various organosilanes and organosilane mixtures. One plot correlated dewetting velocity of a polystyrene thin film as a function of surface energy for both polar and nonpolar surfaces; the other plot consisted of variation of dewetting hole diameters with surface energy for strictly nonpolar surfaces. The empirical plots were then applied to deduce surface energies of micron-scaled areas of gradient and heterogeneous-patterned surfaces. This approach resulted in reasonable values with less than 1% difference as compared to those expected for perfluorodecyl-1*H*,1*H*,2*H*,2*H*-trichlorosilane/*n*-decyltrichlorosilane surfaces. But the difference was slightly higher (35%) for the *n*-octadecyltrichlorosilane (OTS) contact-printed surfaces, which might be a result of better contact with the surface and higher OTS concentration on the stamps when smaller stamps were used.

Introduction

Surface energy determination of a solid is essential when considering surface properties in the areas of wetting/adhesion, friction/lubrication, and surface modification. One common technique for determining the surface energy of a solid/air interface (γ_S) is contact angle measurement,[1−3] which utilizes the angle (θ) at the three-phase contact and the surface energy of a liquid/air interface (γ_L) to estimate γ_S.[4] Recently, contact mechanics, also known as the JKR (Johnson, Kendall, and Roberts) technique,[5] has also been widely adopted for measuring the surface energy of a solid.[6−8] In this technique, a small hemispherical elastomer is brought into contact with the solid surface. As the compressed force acting on the elastomer varies, the contact area between the elastomer and the surface varies accordingly. Thus the surface energy of the solid is obtained from the relationship of the contact area to the compressed force.

The contact angle method is based on the assumption that the surface is homogeneous.[1] Therefore, this method cannot be adequately applied to a surface exhibiting energy variation. One example is a gradient surface, where significant variations of surface energy, in submillimeter scale or less, are present. On such a surface, the three-phase contact line would move continuously toward the higher energy region,[9] and a discrete contact angle would not be obtained. Another example is a heterogeneous surface in which low-energy and high-energy regions are present simultaneously. Multiple contact angles or pinning of the contact lines can result.[10] When the heterogeneity is at the micron scale (i.e., a microcontact-printed surface), contact angle fails to recognize the detailed surface heterogeneity. The droplet, normally having a base diameter of a few millimeters, covers the entire area and exhibits merely the "bulk" contact angle.[11] Studies have shown that heterogeneous surfaces may be analyzed quantitatively using the Cassie equation[12] or a modified Cassie equation.[13] The heterogeneity of a surface can be correlated to the contact angle, which can be estimated based on the fractional area of each component. The analysis, however, is based on a surface whose heterogeneity is known, which is not always true for certain surfaces. Therefore, contact angle measurements may not be suitable for estimating the surface energy of a heterogeneous surface containing unknown components.

In JKR measurements, the contact area, generally circular with a diameter of hundreds of microns,[6] is measured with the aid of an optical microscope. The heterogeneous chemistry of a surface cannot be visualized through an optical microscope. This makes contacting the elastomeric lens in the region of interest very challenging. In addition, the region of interest must have an area greater than hundreds of microns. Therefore, contact mechanics cannot be applied to a surface with micron-scale variations or heterogeneities. Furthermore, for a gradient or heterogeneous surface, the contact area may be distorted and deviate from a circular shape. Neither experimental nor theoretical studies have been performed to address this distortion.

In the search for an alternative to overcome the limitations of contact angle and contact mechanics for surfaces having micron-scale energy variations, the pos-

* Corresponding author.

(1) Andrade, J. D.; Smith, L. M.; Gregonis, D. E. In *Surface and interfacial aspects of biomedical polymers*; Andrade, J. D., Ed.; Plenum Press: New York, 1985; Vol. 1, Chapter 2.
(2) Kinloch, A. J. *Adhesion and Adhesives*: *Science and Technology*; Chapman and Hall: New York, 1987; Chapter 2.
(3) Ulman, A. *An Introduction to Ultrathin Organic Films from Langmuir−Blodgett to Self-Assembly*; Academic Press: San Diego, CA, 1991; Parts 1 and 3.
(4) Adamson, A. W.; Gast, A. P. *Physical Chemistry of Surfaces*, 6th ed.; John Wiley & Sons: New York, 1997; Chapters IV and X.
(5) Pocius, A. V. *Adhesion and Adhesives Technology*: *An Introduction*; Hanser/Gardner: Cincinnati, OH, 1997; Chapter 4.
(6) Chaudhury, M. K.; Whitesides, G. M. *Langmuir* **1991**, *7*, 1013.
(7) Chaudhury, M. K. *J. Adhes. Sci. Technol.* **1993**, *7*, 669.
(8) Chaudhury, M. K.; Owen, M. J. *Langmuir* **1993**, *9*, 29.
(9) Chaudhury, M. K.; Whitesides, G. M. *Science* **1992**, *256*, 1539.
(10) Neumann, A. W.; Good, R. J. *J. Colloid Interface Sci.* **1972**, *38*, 341.
(11) Israelachvili, J. N.; Gee, M. L. *Langmuir* **1989**, *5*, 288.
(12) Cassie, A. B. D. *Discuss. Faraday Soc.* **1952**, *75*, 5041.
(13) Drelich, J.; Miller, J. D. *Langmuir* **1993**, *9*, 619.

10.1021/la026489m CCC: $25.00
Published on Web 01/24/2003

sibility of utilizing the dewetting characteristics of polymer thin films was investigated. The dewetting of a polymer thin film is related to the free energy change of the system, or spreading coefficient[4] ($S_{L/S}$), described as

$$S_{L/S} = \gamma_S - \gamma_L - \gamma_{SL} \quad (1)$$

where γ_S and γ_L denote the surface energies of the substrate/air and the polymer melt/air interfaces, respectively, and γ_{SL} is the polymer/substrate interfacial energy. A polymer melt normally dewets from the substrate when the value of $S_{L/S}$ is negative. Dewetting of polymer thin films is predominantly influenced by surface properties, film thickness, annealing temperature, physical properties of the polymer, and polymer−substrate interactions.[14,15] Sharma and Reiter[16] have interpreted dewetting as a result of the instability induced by long-range forces across the polymer thin film. The long-range forces are inversely proportional to the square of film thickness but directly proportional to the Hamaker constants, which are directly related to the Lifshitz−van der Waals (LW) component of the spreading coefficient ($S^{LW}_{L/S}$). For most nonpolar systems, such as a thin film of polystyrene on a nonpolar surface, $S^{LW}_{L/S}$ is equivalent to $S_{L/S}$. Once the dewetting is initiated, the rate of dewetting can be anticipated and correlated to γ_S. If other experimental parameters are maintained, one correlation plot of the dewetting velocity (V_D) as a function of γ_S and one correlation plot of the dewetting hole diameter (D) at a particular annealing time as a function of γ_S can be generated. These correlation plots can then be used to deduce the value of γ_S by measuring V_D or D of the dewetted polymer thin film from the substrate.

Dewetting of a polystyrene (PS) thin film from surfaces modified with self-assembled monolayers (SAMs) of organosilanes was selected as a model system to generate the correlation plots. Organosilanes having terminal groups of $-CF_3$ or $-CH_3$ were chosen in this study to produce nonpolar surfaces. Two sets of surfaces were prepared: one set contained different surface coverages of CH_3 (octadecyltrichlorosilane, OTS) deposited to the surface using contact printing (CP)[17] in conjunction with varying contact times, while the other set contained various ratios of mixed monolayers of CF_3/CH_3 that were grafted to the surface by vapor phase deposition.[6] Polar surfaces with various γ_S values, using organosilanes containing $-COOH$, $-SH$, $-NH_2$, or $-CH_2Cl$ as the terminal group, were also generated by the solution deposition method.[18]

The surface energy of each model surface was estimated using the contact angle method. Then, a PS thin film was placed on each model surface and allowed to dewet. The D for a nonpolar surface at a particular annealing time and V_D, obtained from dD/dt during the early stages of dewetting, were plotted against γ_S. These plots were then utilized to estimate the surface energies of micron-sized gradients and of heterogeneous organosilane-modified surfaces containing $-CH_3$ and/or $-CF_3$ terminal groups. The contact angle measurement on these surfaces exhibited dubious results. However, by application of the dewetting behavior of PS thin films, γ_S values of the regions of interest were obtained. Although the applications of this technique may be limited to a few organosilane SAM surfaces, it is still a useful tool for surface energy determination in certain technologies such as microelectronics, biotechnology, and nanotechnology, which have widely adopted organosilane SAMs as platform surfaces.[19,20]

Results and Discussion

This research utilized the difference in dewetting behaviors of PS thin films on organosilane-modified surfaces as a means to estimate surface energy. In particular, experiments with model organosilane-modified surfaces were used to generate empirical plots that relate (i) dewetting velocity (V_D) to surface energy (γ_S) and (ii) the diameter of a dewetting hole (D) at a particular annealing time to surface energy. The correlations derived from these plots were then applied to estimate the surface energy of surfaces containing energy gradients or micron-scaled patterns created using organosilanes. The surface energy estimated with this approach was in good agreement with the values that were obtained with contact angle measurements on a large homogeneous surface prepared under the same conditions. In this section, the details associated with generating the correlation plots will be presented. The application of these plots to estimate surface energy on two gradient surfaces and two heterogeneous surfaces will also be discussed.

V_D versus γ_S Using Various OTS Coverages. The first correlation between dewetting velocity of a PS thin film and surface energy was generated using surfaces containing different OTS coverages. The surfaces were generated by contact printing OTS to the surface using different contact times. The scanning probe microscopy (SPM) topographic and lateral force images of the OTS films were examined under ambient conditions to confirm the different OTS coverages (Figure 1). At a contact time of 1 s, OTS molecules were sparsely absorbed throughout the contacted area. At a contact time of 10 s, OTS molecules started to assemble and form small circular islands having average heights of 1.89 nm, which were shorter than the fully extended OTS molecules (2.62 nm[18]). This suggested that the molecules were in a less ordered state.[21−23] Because OTS SAMs had much lower friction than that of the Si/SiO_X substrate,[24] the correspondence of lower friction in the lateral force image to the higher features in the topographic image verified that these islands consisted of OTS molecules. As the contact time increased (up to 30 s), these islands increased slightly in size. The most important observation was the OTS molecule's extension to 2.8 nm, indicating the formation of fully extended OTS molecules. At the same time, secondary islands with sizes similar to those formed with shorter contact times appeared. It was speculated that the secondary island formation was predominated by the diffusion of OTS molecules from the primary islands as in the case of the solution deposition method.[18] As the contact time further increased (up to 60 s), the island

(14) Xie, R.; Karim, A.; Douglas, J. F.; Han, C. C.; Weiss, R. A. *Phys. Rev. Lett.* **1998**, *81*, 1251.
(15) Reiter, G. *Langmuir* **1993**, *9*, 1344.
(16) Sharma, A.; Reiter, G. *J. Colloid Interface Sci.* **1996**, *178*, 383.
(17) Xia, Y.; Whitesides, G. M. *Angew. Chem., Int. Ed.* **1998**, *37*, 550.
(18) Bierbaum, K.; Grunze, M. *Langmuir* **1995**, *11*, 2143.
(19) Zhao, B.; Moore, J. S.; Beebe, D. J. *Science* **2001**, *291*, 1023.
(20) Reyes, D. R.; Iossifidis, D.; Auroux, P.-A.; Manz, A. *Anal. Chem.* **2002**, *74*, 2623.
(21) Wasserman, S. R.; Tao, Y.-T.; Whitesides, G. M. *Langmuir* **1989**, *5*, 1074.
(22) Tillman, N.; Ulman, A.; Schildkrout, J. S.; Penner, T. L. *J. Am. Chem. Soc.* **1988**, *110*, 6136.
(23) Fadeev, A. Y.; McCarthy, T. J. *Langmuir* **2000**, *16*, 7268.
(24) Takahara, A.; Kojio, K.; Kajiyama, T. Aggregation Structure and Surface Properties of Immobilized Polyalkylsiloxane Ultrathin Films Prepared at The Air/Water Interface. In *Fluorinated Surfaces, Coating, and Films*; Castner, D. G., Grainger, D. W., Eds.; ACS Symposium Series 787; American Chemical Society: Washington, DC, 2001; pp 501−502.

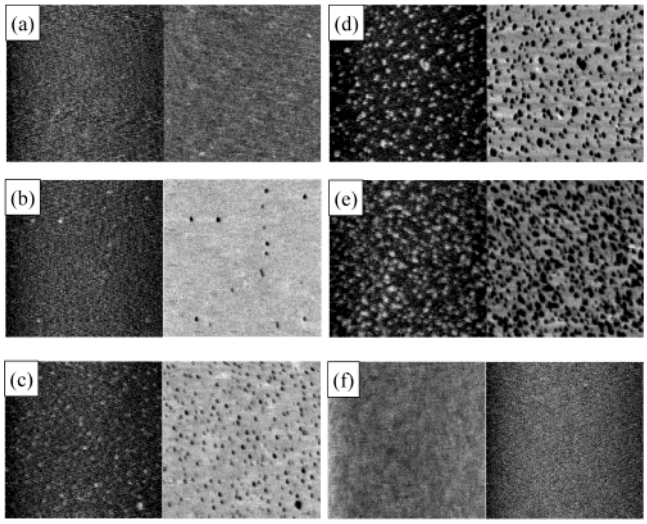

Figure 1. 2 μm × 2 μm SPM topographic and lateral force images of a contact-printed OTS monolayer are presented in the left and right columns, respectively, for each contact time. The higher regions in the topographic images correspond to the lower lateral force regions in the lateral force images, suggesting that these regions were covered with OTS molecules. The OTS domains grew with contact time: (a) with a contact time of 1 s, no visible islands were observed; (b) with a contact time of 10 s, small circular islands (~85 nm diameter) were found; (c) with a contact time of 20 s, the number of small islands was remarkably increased, and secondary islands were also observed among the primary islands; (d) with a contact time of 30 s, the islands grew in size and number; (e) with a contact time of 60 s, the density of islands further increased, but the sizes became comparatively uniform; and (f) with a contact time of 120 s, the islands coalesced and started to form a continuous layer.

density increased with an onset of coalescence. With an extended contact time, more islands coalesced to form a continuous monolayer, even though the Si/SiO_X substrate remained sporadically exposed.

The γ_S of each OTS contact-printed surface was estimated from the contact angles of two probe liquids (liquids 1 and 2) by using the following expressions:[25]

$$1 + \cos\theta_1 = \frac{2(\gamma_S^D\gamma_1^D)^{1/2}}{\gamma_1} + \frac{2(\gamma_S^P\gamma_1^P)^{1/2}}{\gamma_1} \quad (2)$$

$$1 + \cos\theta_2 = \frac{2(\gamma_S^D\gamma_2^D)^{1/2}}{\gamma_2} + \frac{2(\gamma_S^P\gamma_2^P)^{1/2}}{\gamma_2} \quad (3)$$

where γ^D and γ^P represent the dispersion and polar components, respectively. Since γ^D and γ^P values for water (liquid 1) and methylene iodide (MI, liquid 2) could be obtained[2] and contact angles for each liquid were measured, the equations could be simultaneously solved to obtain γ_S^D and γ_S^P, giving a value of $\gamma_S = \gamma_S^D + \gamma_S^P$. The contact angle of each probe liquid used in the above equations was the average of advancing and receding contact angles.

As shown by the surface energies of the OTS contact-printed surfaces in Figure 2, γ_S^P decreased as the contact time increased. Since the majority of γ_S^P was from the polar Si/SiO_X surface, as the contact time increased, more OTS molecules, which consisted of nonpolar $-CH_2-$ chain units and $-CH_3$ terminal groups, were transferred to the substrate, leading to less exposure of the polar Si/SiO_X substrate. However, even with a 120 s contact time,

(25) Good, R. J. *J. Adhes. Sci. Technol.* **1992**, *6*, 1269.

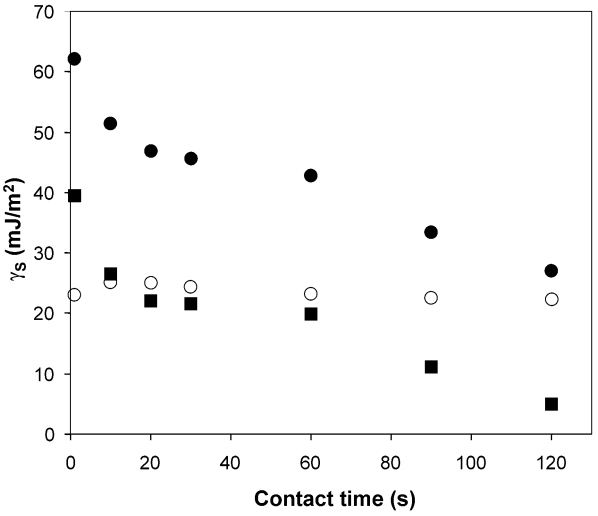

Figure 2. The surface energy (γ_S) and its dispersion (γ_S^D) and polar (γ_S^P) components, represented by ●, ○, and ■, respectively, of the contact-printed OTS at different contact times. As the contact time increased, γ_S^P decreased dramatically, while γ_S^D remained almost constant.

sparsely uncovered Si/SiO_X regions were observed, as the planar stamp (1 cm × 1 cm) may not be in intimate contact with the entire substrate. While γ_S^P showed a dramatic change with the contact time, γ_S^D remained almost constant (around 24 mJ/m^2). In addition, the values of γ^D for $-CH_3$ groups in OTS molecules (21 mJ/m^2)[6] and Si/SiO_X (24.4 mJ/m^2)[26] were similar. Therefore, an increase in OTS coverage might not cause a considerable change in γ_S^D. The fact that the values of γ_S^D at 10 and 20 s contact times were slightly higher than those of other times could be the result of exposure of $-CH_2-$ units (γ^D = 32 mJ/m^2)[27] of the OTS chains, as less-ordered OTS SAMs were expected with these contact times. Although the quality of SAMs (i.e., order) might play a role in the dewetting of polystyrene films, in our studies, this was simply assumed to be reflected in the surface energy that governed the dewetting behavior of the PS thin film.

The dewetting of PS thin films on these OTS surfaces was evaluated. The quality of OTS and the thermal degradation of PS while dewetting at 160 °C in air were initial concerns. However, studies have shown that the OTS monolayer was uniformly consistent after annealing in air[28] at 250 °C but became slightly disordered after annealing at 350 °C for 15 min.[29] The OTS monolayer on Si/SiO_X should be thermally stable for the time scale of our experiment (<60 min). We also performed contact angle measurements on the OTS-modified surface. The contact angles were consistent before and after annealing at 160 °C in air for 1 h, indicating the OTS quality did not change, and thus the surface energy of the OTS-modified substrate remained within the time scale of the dewetting study. Due to the relatively low annealing temperatures

(26) We measured the surface energy (γ_S) of the Si/SiO_X substrate with deionized water, MI, and ethylene glycol (EG) right after UV/O treatment. Water and EG wetted the surface (0°), while MI formed about a 40° angle. Water and MI were used to estimate the γ_S of Si/SiO_X with eqs 3 and 4. The value was about 72.3 mJ/m^2, with the dispersion component of about 24.4 mJ/m^2 and the polar component of about 47.8 mJ/m^2. Since water wetted the surface, the Si/SiO_X more likely had a higher value of the polar component.

(27) Owens, D. K.; Wendt, R. C. *J. Appl. Polym. Sci.* **1969**, *13*, 1741.

(28) Jeon, N. L.; Clem, P.; Jung, D. Y.; Lin, W.; Girolami, G. S.; Payne, D. A.; Nuzzo, R. G. *Adv. Mater.* **1997**, *9*, 891.

(29) Jeon, N. L.; Finnie, K.; Branshaw, K.; Nuzzo, R. G. *Langmuir* **1997**, *13*, 3382.

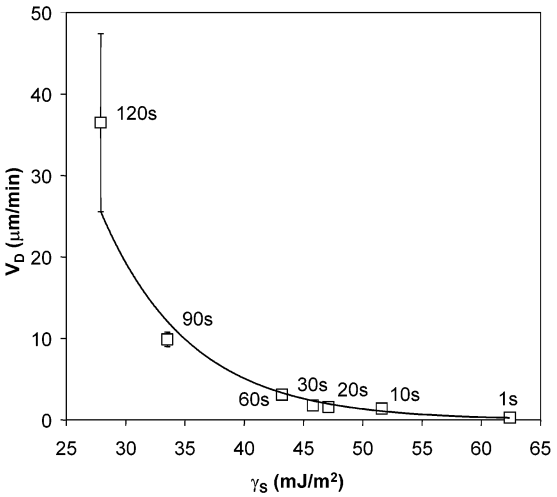

Figure 3. Dewetting velocity, V_D, on contact-printed OTS plotted against γ_S. V_D decreased with the increase of γ_S with an exponential relationship: $V_D \approx 1050 \exp(-0.13\gamma_S)$. The error bars were generated by measuring V_D at different spots of the same type of samples. Errors in V_D for the 1−60 s contact times resided within the symbols.

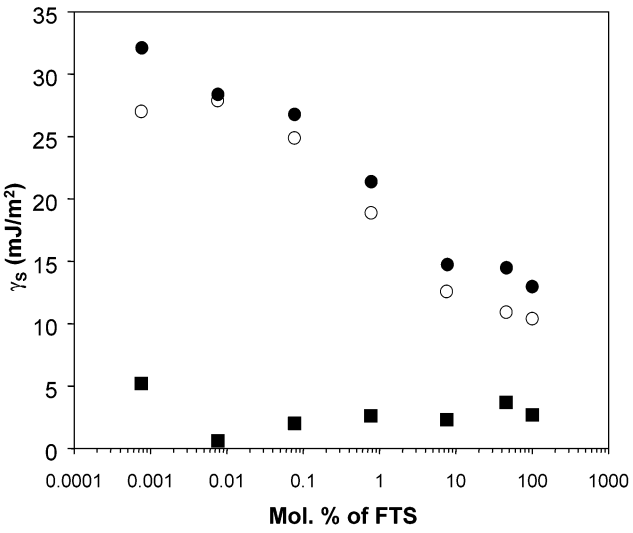

Figure 4. The surface energy (γ_S) and its dispersion (γ_S^D) and polar (γ_S^P) components of the FTS/DTS mixed monolayer generated from vapor phase deposition of FTS and DTS mixtures having different molar ratios are represented by ●, ○, and ■, respectively. To have a more direct comparison to the surface energy estimated using the Cassie equation, the molar ratios instead of the volume ratios were used in this plot. γ_S decreased with the increase of FTS content, which had a lower γ_S than that of DTS. γ_S measured on the mixed monolayer did not vary linearly with the molar ratios of the predeposited FTS/DTS solutions. As DTS content decreased, γ_S^P fluctuated more or less around a certain constant value, while γ_S^D decreased noticeably.

and short annealing process, thermal degradation of PS, if it happened, would likely play a much smaller role in the dewetting as compared to the surface energy effects.

The dewetting process varied from a few minutes to 1 h depending on the dewetting behavior of a particular surface. For samples with more than a 20 s contact time, PS thin films dewetted rapidly, leading to the coalescence of dewetting holes within a few minutes. However, for 1 and 10 s contact times, the hole growth slowed and reached a plateau before holes were able to contact each other. Dewetting velocity was chosen as the linear growth period. It occurred for longer contact-printed samples prior to hole coalescence and for shorter contact-printed samples when hole growth leveled off. Hole growth was found to be relatively uniform throughout the surface for each OTS contact-printed surface. The V_D was the average value of V_D measured from several spots on each OTS contact-printed surface. At least two OTS surfaces having the same contact times were used. Figure 3 summarizes the variation of V_D as a function of γ_S. The overall trend expressed an exponential relationship with an exponent of $-0.13\gamma_S$ and a coefficient of 1050. The large standard deviation of V_D at the 120 s contact time may originate from the dramatic change of V_D on the slight variation of γ_S of the three surfaces used. Experiments showed that V_D was very sensitive to γ_S in the low-γ_S region.

V_D versus γ_S Using Mixed FTS/DTS Monolayers. Another set of nonpolar surfaces with different surface energies was generated by vapor phase depositing[6] mixtures of perfluorodecyl-1*H*,1*H*,2*H*,2*H*-trichlorosilane (FTS)/*n*-decyltrichlorosilane (DTS) with various volume fractions of the components. The thermal stability of the FTS/DTS mixed monolayer was first examined by measuring contact angles after heating the FTS/DTS-modified surfaces at 160 °C for several hours. The contact angles observed were consistent with the contact angles before heating. Since FTS and DTS had matching chain lengths, any topographical effect from the chain length difference within the monolayer[30] that might affect the dewetting process could be minimized. The SPM observations for the FTS/DTS monolayer confirmed no noticeable height difference. The scan size was varied from 200 nm × 200 nm to 10 μm × 10 μm. Lateral force and phase images of SPM, revealing frictional and mechanical properties of the monolayer, respectively, were also utilized to qualitatively discern possible phase separation of FTS and DTS in each mixed monolayer. The phase-separated FTS and DTS might affect the dewetting of PS thin films differently as compared to the homogeneous mixed FTS/DTS monolayer. FTS chains likely form helical structures, whereas DTS chains are normally in a planar zigzag structure. C−C bonds would encounter more resistance in rotating with the helical conformation than with the planar zigzag formation. As a result, the frictional force of FTS would be much higher than that of DTS.[31−32] Also, stretching or compressing of CF_2-CF_2 bonds due to the rotational barrier and the helical conformation should be harder than that of CH_2-CH_2 bonds. If phase separation were to occur, it should be observed in those images. The frictional force and phase images of the mixed SAMs revealed no clear evidence of prominent phase separation, such as the formation of domains on the micron scale.

The γ_S and its components (γ_S^D and γ_S^P) presented in Figure 4 were calculated from eqs 2 and 3. The γ_S decreased as the FTS content increased, since the surface consisting of $-CF_3$ terminal groups ($\gamma_S = 10.4$ mJ/m^2) had a much lower surface energy than that of the $-CH_3$ terminal groups ($\gamma_S = 21$ mJ/m^2).[6] In contrast to Figure 2, γ_S^D changed dramatically while γ_S^P remained constant with a value of ~2.7 mJ/m^2. The surface energy of both FTS and DTS was composed mostly of γ_S^D. However, the presence of a polar component in the FTS/DTS mixed monolayer was not totally unexpected. One possibility for this

(30) Beake, B. D.; Leggett, G. J. *Phys. Chem. Chem. Phys.* **1999**, *1*, 3345.

(31) Song, K.; Hallmark, V. M.; Rabolt, J. F. *J. Chem. Phys.* **1991**, *95*, 2826.

(32) Shin, S.; Collazo, N.; Rice, S. A. *J. Chem. Phys.* **1991**, *95*, 2862.

occurrence was the defects in the mixed monolayer or incomplete coverage of the monolayer, resulting in a slight exposure of the Si/SiO_X substrate. Another possibility was the strong electronegativity of fluorine present in FTS which might have the ability to form hydrogen bonds with water[28] and contribute to the γ_S^P.

The resulting γ_S (Figure 4) did not correlate directly to the compositions of the original FTS/DTS mixtures. According to Cassie's equation,[12] a linear correlation between the resulting contact angle and the compositions of the original mixture would be expected if the monolayer had the same composition as the predeposited mixture. As a result, γ_S of the mixed monolayer, estimated from the θ derived from Cassie's equation, should be nearly linear over the entire composition of the mixtures. The experimentally measured γ_S of the mixed monolayer on a silicon wafer showed FTS domination. It was found that γ_S of the mixed-monolayer-modified substrate was inversely proportional to the logarithm of the FTS fraction with a slope of about −4. This suggested that the $-CF_3$-terminated organosilane, or FTS, might be preferentially deposited onto the substrate and/or more easily detected.

The possible preferential adsorption of FTS was therefore evaluated. The possible causes from our experimental procedures were eliminated first. On the basis of the higher molecular weight, boiling point, and density of FTS molecules, FTS was less volatile than DTS. As a result, more DTS molecules could be vaporized during the degassing process, leaving insufficient amounts for the deposition process. If this were true, then γ_S of the surface modified with the FTS/DTS 50/50 v/v mixture without degassing should have been higher (due to more DTS molecules) than that of the degassed mixture. We conducted separate experiments of FTS/DTS 50/50 v/v without degassing, and γ_S of the respective modified surface was still similar to the result of the degassed sample (∼13.1 mJ/m^2). Therefore, the preferential adsorption was not simply the result of the experimental treatment. On the basis of the higher values of γ_S^D and γ_S^P of our DTS surface as compared to the closely packed DTS, our DTS formed a disordered, liquidlike structure. The disorder of DTS, probably due to the presence of gauche bonds, could cause a slight shortening of the chain length.[33] This shortening then could lead to the preferential adsorption of relatively longer FTS molecules, as in the case of mixed thiols.[34] Also, it was reported that the polarity of the component drives its preferential adsorption.[35] FTS molecules, containing highly polarizable fluorine, were more polar than DTS molecules.

In addition to the preferential adsorption, the arrangement of the FTS and DTS molecules in the mixed monolayer could reveal the preference of FTS over DTS. This could be the combined result of the slightly shorter chain length and smaller terminal group of DTS. The slight shortening of the DTS molecules due to the existence of gauche bonds and the disordered monolayer caused the $-CH_3$ terminal groups to be positioned underneath the $-CF_3$ terminal groups (Figure 5). The FTS molecules could "stand straight" by virtue of the intramolecular stabilization of the rigid rodlike helical structure of fluorocarbon chains.[36] The larger $-CF_3$ terminal groups acted as "an umbrella" in preventing the probe liquids from penetrating

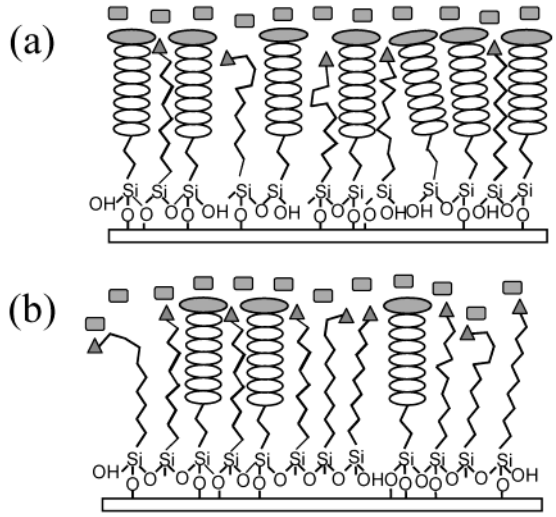

Figure 5. An illustration of the interaction between probe liquid molecules (denoted as the rounded rectangles) and the FTS/DTS mixed monolayer formed on the Si/SiO_X substrate. The 3-D cross-polymerization among the organosilane molecules and the covalent bonding between the organosilane molecules and the substrate were simplified. (a) With higher contents of FTS (FTS/DTS 50/50 or 10/90 v/v), the probe liquid molecules mainly interacted with FTS molecules due to the molecular arrangement of FTS (represented by a helical structure and an elliptical terminal group) and DTS (represented by zigzag chains and triangular end groups), the disordered monolayer structure of DTS, and the possible preferential adsorption of FTS molecules. (b) With lower FTS contents (FTS/DTS ≤ 1/99), DTS molecules formed a dominant continuous phase and FTS molecules were isolated. As a result, probe liquids sensed both the FTS and DTS molecules.

and reaching the underlying $-CH_3$ groups at high contents of FTS (50 vol % and 10 vol % of the original mixture). We roughly calculated the projected area of a single $-CH_3$ and $-CF_3$ group from their van der Waals hemisphere volumes.[37] The areas occupied by $-CF_3$ and $-CH_3$ were ∼23.4 and ∼12.6 $Å^2$, respectively. Therefore, more direct contact of the probe liquids with $-CF_3$ groups contributed to the measured γ_S. For DTS molecules to be detected, a significant amount of DTS molecules on the substrate was needed. Experimentally, only concentrations of ≥99 vol % DTS resulted in γ_S measurements with a $-CH_3$ contribution.

The correlation plot of V_D versus γ_S in the case of FTS/DTS mixed monolayers is presented in Figure 6. As before, the relationship was not linear but exhibited an exponential trend with an exponent of $-0.10\gamma_S$ and a coefficient of 620. The relatively poor alignment of the data to the fitted line could be the result of difficulties in reproducing the dewetting process, as the data were collected from at least three sets of surfaces over 12 months. The variation was attributed to nuisance factors such as environmental parameters. Ambient conditions have been shown to affect the monolayer formation.[23] However, precise control of the ambient conditions during each deposition and dewetting experiment was difficult.

V_D versus γ_S Using Polar Organosilane Surfaces. The correlation of V_D and γ_S toward polar organosilane surfaces was also investigated by generating surfaces using 3-aminopropyltriethoxysilane (APTES, $-NH_2$), 2-(carboxymethylthio)ethyltrimethylsilane (CTMES, −COOH), 3-chloropropyltrimethoxysilane (CPTMOS, $-CH_2Cl$), and 3-mercaptopropyltrimethoxysilane (MPT-

(33) Tsao, M.-W.; Rabolt, J. F.; Schonherr, H.; Castner, D. G. *Langmuir* **2000**, *16*, 1734.
(34) Bain, C. D.; Whitesides, G. M. *J. Am. Chem. Soc.* **1989**, *111*, 7164.
(35) Pankewitsch, T.; Vanhoora, P.; Jerome, R.; Stamm, M. *Macromolecules* **1995**, *28*, 6986.
(36) Rabolt, J. F.; Fanconi, B. *Polymer* **1977**, *18*, 1258.
(37) Bott, G.; Field, L. D.; Sternhill, S. *J. Am. Chem. Soc.* **1980**, *102*, 5618.

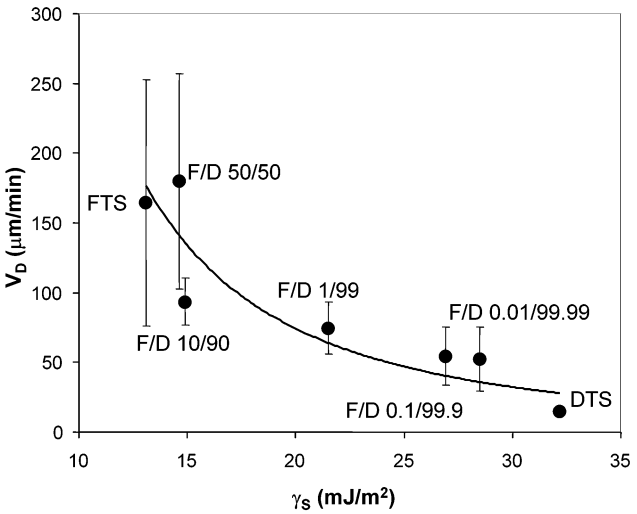

Figure 6. V_D of a PS thin film on a FTS/DTS mixed monolayer was plotted versus γ_S. The trend line showed a relationship of $V_D \approx 620 \exp(-0.10\gamma_S)$. The error bars were generated from measuring V_D at different spots of the sample.

MOS, −SH) with the solution deposition method.[18] However, data obtained over the polar surfaces were scattered with no discernible trend. The polar terminal groups may have induced interactions (e.g., strong hydrogen bonding between −COOH or $-NH_2$ and water molecules) with the probe liquids, which likely resulted in the deviated γ_S. The polar surface activity could also cause fast contamination by adsorbing airborne particles, moisture, and organic debris, thus altering the exact γ_S value of the surface.[38,39]

On the basis of the significantly large water contact angle hysteresis (∼30° for APTES and ∼20° for the other polar silanes, CTMES, MPTMOS, and CPTMOS), the polar organosilanes might have failed to form close-packed or complete SAMs. The polar organosilanes used in this study only had two or three alkyl units in their backbones. The short alkyl chain (<4 CH_2) probably caused the molecules to form a disordered or an incomplete monolayer.[21−23] In addition, APTES is known to form multilayers using the solution deposition method,[40] resulting from 3-D polysiloxane networks having many possible molecular conformations and orientations.[41] This incomplete monolayer or random multilayer formation of the polar organosilanes could perturb the sole contribution of γ_S to dewetting behaviors. To verify the quality of the monolayer, we obtained surface root-mean-square roughness values, R_q, from the topographic SPM images of the organosilane surfaces. The surface roughness provides a crude insight on the homogeneity of a surface. All of the organosilane surfaces generated were scanned. The value of R_q was estimated by averaging several scans with different scan sizes of the same type of surfaces. We were aware that the values were subject to change for the same sample type depending on the sensitivity of SPM (e.g., scan mode, tip condition, vibration). The scans were performed under well-controlled conditions and procedures, and the overall trend for different organosilanes was found to be similar within each scan set. The polar surfaces had relatively higher values of R_q than did the nonpolar FTS/DTS surfaces, indicating that the polar surfaces were more likely incomplete and/or multilayer.

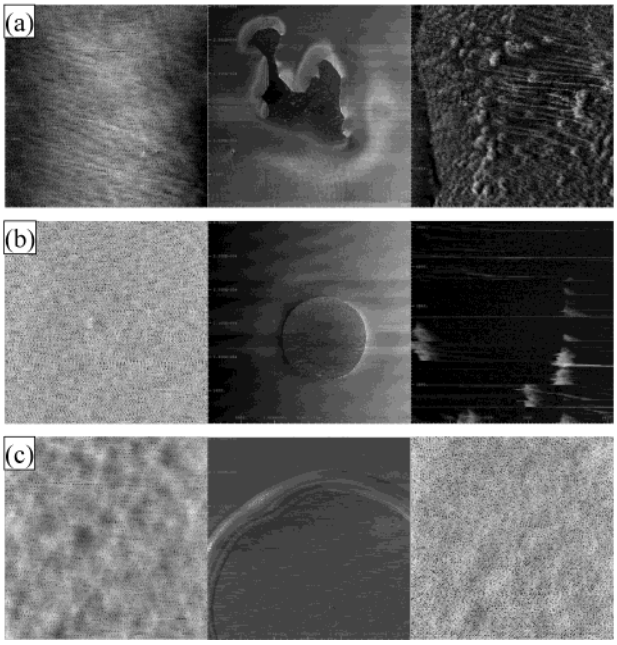

Figure 7. Selected lateral force images of the organosilanes: (a) APTES, (b) SiO_X, and (c) 120 s contact-printed OTS. The images from left to right are the organosilane surface (2 μm × 2 μm) before placing a PS thin film, a dewetting hole of the PS thin film (30 μm × 30 μm) from the surface, and the floor of the dewetting hole (5 μm × 5 μm). Residual polymers were detected on the dewetted floor of APTES and SiO_X, but not on the dewetted floor of OTS.

The polar terminal groups could also interact with PS molecules during the dewetting process, hence complicating the dewetting behaviors of the polymer thin film. APTES had been widely used as an adhesion promoter.[40] The markedly low V_D on the APTES surface implied that the $-NH_2$ terminal group could strongly affect the dewetting behavior. The polar organosilanes could have higher friction[42] and adhesion forces, which could interfere with the dewetting process. Likewise, other unrevealed interactions between PS and the other polar organosilanes could exist. The floor of dewetting holes was also scanned with SPM lateral force imaging (Figure 7), since it is believed that the lateral force imaging is more sensitive than the topographic imaging for detecting the presence of PS residuals. The dewetting holes from all polar surfaces had detectable nuclei, which initiated the dewetting, and patches of residual materials. This indirectly indicated an interaction between the PS thin film and the polar surface that prevented the PS thin film from dewetting. The scans showed that dewetting holes from the APTES surface had irregular shapes. In addition, the floor of the hole was left with a significant amount of PS residuals (Figure 7a). The dewetted hole floor from the Si/SiO_X also showed a small amount of PS residuals (Figure 7b). Conversely, the floor of the dewetted hole from the OTS or FTS/DTS surface was very smooth with no noticeable features (Figure 7c). This was direct evidence that certain properties of polar surfaces, other than γ_S, hindered the dewetting process.

Master Plot of V_D versus γ_S on Organosilane Surfaces. A master correlation between V_D versus γ_S for

(38) Holmes-Farley, S. R.; Bain, C. D.; Whitesides, G. M. *Langmuir* **1988**, *4*, 921.
(39) Drelich, J.; Wilbur, J. L.; Miller, J. D.; Whitesides, G. M. *Langmuir* **1996**, *12*, 1913.
(40) Heiney, P. A.; Gruneberg, K.; Fang, J.; Dulcey, C.; Shashidhar, R. *Langmuir* **2000**, *16*, 2651.
(41) Sudholter, E. J. R.; Huis, R.; Hays, G. R.; Alma, N. C. M. *J. Colloid Interface Sci.* **1985**, *103*, 554.
(42) Brewer, N. J.; Beake, B. D.; Leggett, G. J. *Langmuir* **2001**, *17*, 1970.

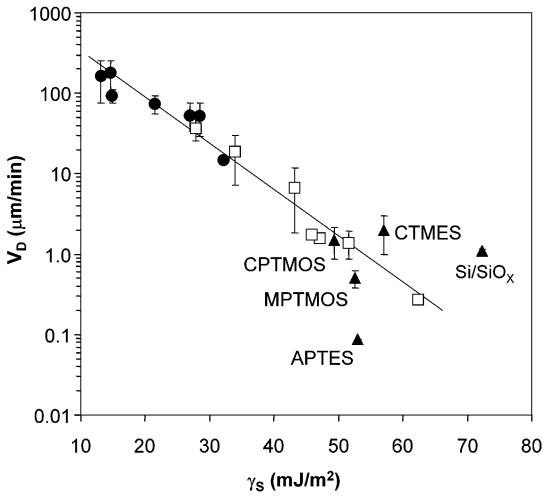

Figure 8. V_D of a PS thin film plotted against γ_S of all the organosilane surfaces used in this study: (i) vapor phase deposition of different volume ratios of FTS/DTS mixtures (●), (ii) CP of the OTS monolayer with various contact times (□), and (iii) solution deposition of polar organosilanes (APTES, CTMES, CPTMOS, and MPTMOS) (▲). An overall correlation between V_D and γ_S could not be obtained due to the dispersity of data for the polar organosiloxane surfaces. When only the nonpolar surfaces were chosen, an overall correlation had a relationship of $V_D \approx 1200 \exp(-0.13\gamma_S)$.

various organosilane surfaces was attempted in order to combine the data obtained from both the nonpolar (various OTS coverage surfaces and the FTS/DTS mixed surface) and the polar surfaces (Figure 8). However, data on the polar surface diverged from the fitted line of data on the nonpolar surfaces. The divergence was not surprising, since other factors could contribute to the dewetting of the PS thin film from polar surfaces. Therefore, the polar organosilane surfaces might not be suitable for inclusion in the correlation between V_D and γ_S. For all the nonpolar surfaces described above, an overall expression of $V_D \approx 1200 \exp(-0.13\gamma_S)$ was obtained.

Correlation Plot of *D* versus γ_S on Organosilane-Modified Surfaces. PS thin films dewet rapidly on some low-energy and nonpolar surfaces modified by organosilanes. On a uniformly covered OTS surface, the entire dewetting process (starting from initiation of the hole and ending with hole coalescence and droplet formation) occurred within 5 min upon annealing at 160 °C. On the FTS-modified surfaces, since the surface energy is lower, the initiated holes grew and coalesced within 2 min upon annealing at 160 °C. If a gradient surface resulted from a surface containing a gradual variation of OTS coverage, the dewetting of a PS thin film at different regions could be difficult to follow. A low-magnification objective could cover more regions of the gradient surface, but the dewetting holes would be too small to be measured, whereas a higher magnification could provide clearer images of the dewetting holes. However, due to the rapid dewetting process, the sample must constantly be repositioned and be refocused in order to follow the growth of various dewetting holes in different regions. Following the dewetting hole growth of a PS thin film on a surface consisting of micron-scaled heterogeneity created using OTS or FTS has two challenging tasks. One challenge is to locate the exact regions of the micron-scaled heterogeneity during the early stages of dewetting when the hole growth is linear. The other challenge is to view all the heterogeneous regions simultaneously. Hence, the correlation of hole diameter (D) versus surface energy (γ_S) after a particular annealing time was generated as another means of backtracking γ_S. To achieve this, the dewetting hole diameter of the PS thin film was experimentally measured after annealing at 160 °C for 1 min on each of the OTS contact-printed (from 1 to 120 s contact times) surfaces (Figure 9) or 15 s on the FTS/DTS-modified surfaces (not shown). These surfaces were the same as those described in the preceding sections. The correlation was then plotted against γ_S. For the surface that was OTS contact printed alone, a relationship of $D \sim 7 \times 10^9 \gamma_S^{-5.8}$ was observed. The FTS/DTS surfaces had a relationship of $D \sim 8.6 \times 10^3 \gamma_S^{-2.1}$.

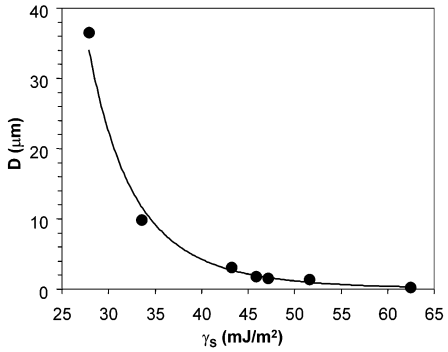

Figure 9. The correlation plot of dewetting hole diameter (D) versus γ_S of the contact-printed OTS surfaces. D was obtained from the PS thin film dewetted from each contact-printed OTS (from 1 to 120 s contact time) surface after the sample was annealed at 160 °C in ambient conditions for 1 min. With 1 min of annealing, D varied with γ_S to a power-law relationship of $D \sim 7 \times 10^9 \gamma_S^{-5.8}$. This plot allowed us to deduce the surface energy of the OTS contact-printed surface by measuring the hole diameter at a particular annealing time (1 min in this case).

Surface Energy Determination of Gradient and Heterogeneous Surfaces. We applied the correlation plots to determine surface energy of four sample surfaces. The first two samples were OTS gradient surfaces with different gradient scales, the third sample was a heterogeneous surface containing micron-sized alternating stripes of OTS and SiO$_X$, and the fourth sample was a heterogeneous surface containing millimeter and submillimeter alternating stripes of a FTS/DTS mixed monolayer and SiO$_X$. The gradient surfaces were generated using contact printing of OTS from a hemispherical silicone stamp that allowed gradual stamping and differentiated contact times as the contacted area increased. According to the above findings (Figures 1 and 2), contact time was directly related to γ_S.

The contact angle measurements using water as the probe were first attempted to verify the gradient prior to the dewetting process. Depending on the gradient steepness or scale, the behavior of water varied: pinning of water, asymmetric water droplets, sudden movement of water droplets from the low-energy region toward the high-energy region, and irregularity of contact lines. Therefore, no static contact angles could be obtained with the sessile drop method.

Dewetting of PS films on the gradient surfaces was then conducted. The gradient surfaces were generated by contact printing OTS to a cleaned and oxidized SiO$_X$ surface, with a gradual decrease of contact time from 60 to 1 s. When the gradient was measured over several millimeters, it was difficult to simultaneously follow the growth of dewetting holes over the entire surface with an optical microscope in real time. Therefore, the correlation plot of D versus γ_S was utilized for determining γ_S. The PS films were placed onto the gradient surfaces and treated with the same procedure as those on the silanized surfaces.

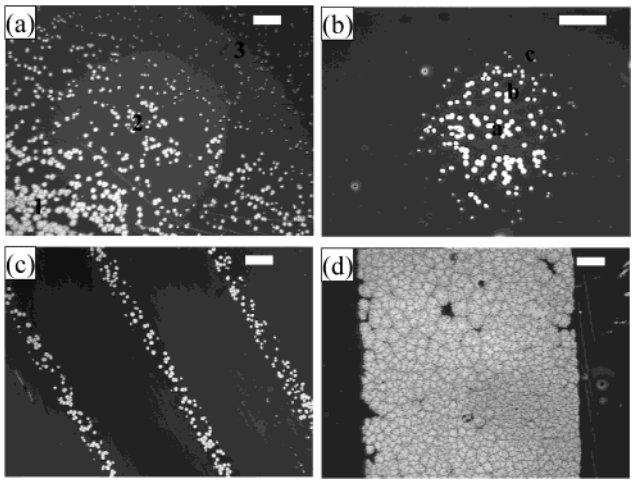

Figure 10. Optical microscope images of the PS thin film dewetted from gradient and heterogeneous surfaces. Two gradient surfaces, (a) and (b), were generated by CP of OTS using a hemispherical stamp having a radius of ~20 and ~2 mm, respectively. The micron-scale heterogeneous surface (c) was generated by μ-CP of OTS on Si/SiO_X. The larger scale heterogeneous surface (d) was generated by selective UV/O oxidation of the FTS/DTS 0.1/99.9 mixed monolayer. For surfaces containing OTS, the film was annealed at 160 °C in ambient conditions for ~1 min, whereas for the FTS/DTS surface, the annealing time was ~45 s. The scale bars are 200 μm in all the images.

Then the samples were annealed at 160 °C for 1 min, followed by quenching to room temperature to preserve the dewetted hole morphology. Two representative dewetted images of gradient surfaces, shown in Figure 10a,b, were generated using hemispherical stamps having radii of ~20 and ~2 mm, respectively. The diameter of the dewetting holes decreased from the center toward the edges. The γ_S values, deduced using Figure 9, for three different regions located from the center to the edge, indicated as 1, 2, and 3 in Figure 10a, were 27.1, 30.5, and 35.8 mJ/m^2, respectively. The surface energies for positions a, b, and c of Figure 10b were estimated to be 29.2, 31.3, and 35.4 mJ/m^2, respectively. The surface energies were lower than the values obtained from the contact-printed OTS surfaces with corresponding contact times using planar stamps. This could be the result of better contact with a smaller contact area and a possible higher concentration of OTS accumulated at the center of the hemispherical stamp. Therefore, utilizing the dewetting of PS thin films, the γ_S on gradient surfaces generated with contact printing of OTS could be successfully estimated.

Heterogeneous surfaces were created with microcontact printing (μ-CP)[17] of OTS and selective oxidation of the FTS/DTS mixed monolayer. For μ-CP of OTS, an elastomeric poly(dimethylsiloxane) (PDMS) stamp having embossed stripes with a width of ~150 μm and a spacing of ~600 μm was used. We attempted contact angle measurements with water on the contact-printed area to verify feasibility of contact angle measurements on a heterogeneous surface. Water, extended only on Si/SiO_X regions, formed remarkably irregular three-phase contact lines, which became even more contorted when the heterogeneity was at the micron scale.[43] Therefore, true contact angles could not be obtained on surfaces with micron-scaled heterogeneities. Alternatively, by application of dewetting studies of the PS thin film, the width of the stripes was found to be around 130−140 μm with spacings of ~610 μm (Figure 10c). The values were in good agreement with the original spacing of the stamp. γ_S of the stripes was deduced from Figures 3 and 8 with V_D and Figure 9 with D (averaged using several holes) after 1 min of annealing. The deduced γ_S values from all the plots showed an averaged value of 27.0 ± 1.4 mJ/m^2. Again, the γ_S of microcontact-printed OTS for 60 s was lower than the value of 60 s contact-printed OTS using a planar stamp. As mentioned earlier, the reasons could probably be a better contact and a higher OTS concentration on the thin stripes as compared to conditions for a large planar stamp. We were also able to estimate γ_S of stripes with sizes of tens of microns with this method.

Heterogeneous-patterned surfaces of FTS/DTS mixed monolayers were achieved by masking the desired regions with Scotch tape and removing the unmasked mixed monolayer with UV/O oxidization. Contact angle measurements with water showed similar behavior and results to those for the heterogeneous surface generated using μ-CP of OTS. The formation of a water film only on the unmasked stripes after dipping into a water bath also verified the generation of SiO_X stripes. After placement of the PS thin film on the surface, the V_D of the masked area was measured for each sample (FTS/DTS mixed monolayers with the volume ratios of 0.1/99.9 and 50/50). The γ_S of each FTD/DTS surface was deduced from both Figures 6 and 8, and the values were in good agreement with each other. The γ_S values of FTS/DTS stripes with the ratios of 0.1/99.9 and 50/50 were 26.8 ± 2.6 and 13.1 ± 1.8 mJ/m^2, respectively. These agreed very well with the values obtained from the homogeneous surface of each mixture using the contact angle method. Therefore, for a surface consisting of micron-scaled heterogeneity, the γ_S of the area can be estimated by applying the dewetting study and the correlation plots generated in this study.

Concluding Remarks

The characterization of organosilane-modified surfaces has become vitally important, due to their wide utilization in the areas of microelectronics, biotechnology, and nanotechnology. In microelectronics and nanotechnology, organosilanes are applied as resist layers for generating micron- or submicron-sized features. In biotechnology, gradient surfaces generated with organosilanes are utilized to study the subtle variations of surface properties on protein adsorption and cell attachment and growth. One of the most crucial surface properties for these applications is the surface energy. Common techniques, such as contact angle and contact mechanics, are almost impossible to use in estimating surface energy of micron-sized areas or surface energy variation at the micron scale. A reasonable contact angle would fail to form on the micron-sized heterogeneous surface and the gradient surface due to the complicated contortion and the continuous movement of the three-phase contact line, respectively. Therefore, a new technique needs to be developed.

In this study, we explored the dewetting of polymer thin films as a means for surface energy determination. In particular, two correlation plots were generated, one describing the dewetting velocity of a polystyrene thin film as a function of surface energy for nonpolar surfaces and the other consisting of the variation of dewetting hole diameter with surface energy for nonpolar surfaces at a particular annealing time. The surface energy was varied by modifying a silicon wafer through μ-CP of OTS under different contact times or using mixed SAMs with different ratios of $-CF_3$- and $-CH_3$-terminated organosilanes. Polar

(43) Good, R. J.; Koo, M. N. *J. Colloid Interface Sci.* **1979**, *71*, 283.

surfaces with $-COOH$-, $-CH_2Cl$-, $-NH_2$-, and $-SH$-terminated groups were also generated. However, these surfaces involved other complicated factors on dewetting behaviors of polymer thin films. As a result, a simple correlation of dewetting velocity versus surface energy could not be obtained. We, therefore, concentrated our efforts on the nonpolar organosilane surfaces. For nonpolar surfaces, the overall relationship of $V_D \approx 1200 \exp(-0.13\gamma_S)$ was obtained. The plot of dewetting hole diameter after 1 min of annealing versus surface energy exhibited a power-law relationship of $D \sim 7 \times 10^9 \gamma_S^{-5.8}$. The surface energies of gradient surfaces and surfaces containing micron-scaled heterogeneous patterns could be deduced from the correlation plots using the dewetting of polystyrene thin films on these surfaces.

Our alternative surface energy determination method provides several additional advantages. The entire surface characteristics, mainly surface energy, can be roughly visualized (surface mapped) by dewetted holes and the rate of dewetting. This provides a possible window into a crude insight of surface chemistry without complicated analytical instrumentation (IR, X-ray photoelectron spectroscopy, X-ray reflectivity). The estimated surface energy can be applied for further quantitative investigation of adhesion, friction, and lubrication. By variation of the polymer, film thickness, and annealing temperature, more effective and adequate dewetting velocity versus surface energy plots may be generated for particular systems of interest.

Experimental Section

Materials and Equipment. The organosilanes, perfluorodecyl-1*H*,1*H*,2*H*,2*H*-trichlorosilane ($CF_3(CF_2)_7(CH_2)_2SiCl_3$), *n*-decyltrichlorosilane ($CH_3(CH_2)_9SiCl_3$), *n*-octadecyltrichlorosilane ($CH_3(CH_2)_{17}SiCl_3$), 3-aminopropyltriethoxysilane ($H_2N(CH_2)_3Si(OC_2H_5)_3$), 2-(carboxymethylthio)ethyltrimethylsilane ($HOOCCH_2S(CH_2)_2Si(CH_3)_3$), 3-chloropropyltrimethoxysilane ($ClCH_2(CH_2)_2Si(OCH_3)_3$), and 3-mercaptopropyltrimethoxysilane ($HS(CH_2)_3Si(OCH_3)_3$) were obtained from Gelest, Inc., and used as received. The organosilanes were sealed with Parafilm and stored inside a vacuum and dry desiccator prior to use to minimize possible irreversible hydrolysis. Polystyrene ($M_w = 65\,000$, PI = 1.03) was purchased from Polymer Source. Sylgard 184 (both base elastomer and curing agent) was the source of silicone elastomer (poly(dimethylsiloxane)) used for fabricating the stamps. It was purchased from Dow Corning Corp. The substrates used were 4 in. test silicon wafers of P(1,0,0) purchased from Silicon Quest International.

Sample Preparation. *Substrate Cleaning.* Silicon wafers were cut into 1 cm × 1 cm pieces. The substrates were cleaned by immersing in a freshly prepared piranha solution (70/30 (v/v) of concentrated H_2SO_4 and 30% H_2O_2) for 1 h.[44] The solution was decanted, and the substrates were rinsed thoroughly with deionized water. The cleaned substrates were dried under a stream of N_2 gas and then exposed to UV/ozone (UV/O cleaner model 42, Jelight) oxidization for 6 min immediately prior to the deposition of organosilanes. The entire cleaning process provided silicon wafers with clean and oxidized surfaces containing mainly Si−OH groups.

Stamp Fabrication. The stamps were fabricated from silicone elastomer. The elastomer was generated by mixing the Sylgard 184 elastomer base and curing agent according to the prescribed recipe. The mixture was then poured into a plastic weighing dish containing a master template placed on the bottom of the dish. For stamps with a completely flat surface, the master was a piece of silicon wafer treated with FTS (as described below). For stamps containing patterns, a master bearing micron-scaled strips in sizes of tens to hundreds of microns was used. After the mixture was cured at room temperature for 48 h, the elastomeric stamps were peeled away from the masters. A large hemispherical stamp (radius of curvature ~ 20 mm) was generated by pouring the uncured PDMS mixture into a FTS-treated disposable test tube with a round bottom. Smaller stamps (radius of curvature ~ 2 mm) were generated by placing droplets of the uncured PDMS mixture from a micropipet on FTS-treated silicon wafers. The mixture was again allowed to cure at room temperature for 48 h and removed from the host. All the fabricated stamps were extracted with a Soxhlet extractor in toluene for 2 h to remove un-cross-linked PDMS chains.

Contact Printing of OTS. For contact printing of OTS onto a silicon wafer, a cotton swab was dipped into a 2 mM solution of OTS in HPLC-grade hexane. The solution was applied onto the planar silicone stamp by rubbing the cotton swab on the flat surface. The inked stamp was then dried with a stream of N_2 to remove the solvent. After drying, the stamp was brought into contact with the cleaned and oxidized silicon wafer for various lengths of time (1, 10, 20, 30, 60, 90, and 120 s) under finger pressure and removed. Each stamped silicon wafer was stored in a glass Petri dish at room temperature for 1 h to provide sufficient time for OTS molecules to react with the silicon wafer. Then, it was sonicated in toluene inside an ultrasonic cleaner (model 50HT, Aquasonic) for 2 min. The OTS-modified substrates were then dried with N_2 gas and characterized within 4 h. This exact procedure was followed for each sample.

Vapor Phase Deposition (VPD) of Mixed Organosilanes. Mixtures of FTS and DTS with various volume ratios were used. For each volume ratio, 200 μL of organosilane mixture in 3 g of mineral oil was thoroughly mixed, poured into a plastic weighing dish, and placed inside an empty glass desiccator. The desiccator was vacuumed to a pressure of ca. 10 mTorr and maintained at that pressure for 20 min to remove the trapped air bubbles in the solution. Then, a glass slide, on which the cleaned and oxidized silicon wafers were attached face down using a double-sided Scotch tape, was laid across the plastic weighing dish approximately 1 cm above the degassed solution. The assembly was vacuumed again to the same pressure and maintained for 1 h. After the organosilane-treated silicon wafers were removed from the desiccator, they were thoroughly rinsed with freshly distilled toluene inside a Soxhlet extractor for 1 h. The samples were then dried with N_2 gas and characterized within 4 h.

Solution Deposition of Polar Organosilanes. Polar organosilanes, APTES, CTMES, CPTMOS, and MPTMOS, were deposited to the cleaned and oxidized silicon wafer using the most common solution deposition method.[18] Clean silicon wafers, as described above, were placed in a 2 mM solution of each polar organosilane in HPLC-grade hexane. The chemisorption of the polar organosilanes was allowed to occur for 1 h at room temperature. The modified substrates were removed from the solution and rinsed in a Soxhlet extractor for 1 h using toluene. The samples were then dried under N_2 and stored in plastic Petri dishes prior to characterization, which is normally conducted within 4 h after deposition.

Gradient Surfaces and Heterogeneous Surfaces. Gradient surfaces were generated by bringing hemispherical stamps (centimeter and millimeter scale), inked with OTS, into contact with a cleaned and oxidized silicon wafer and then gradually increasing the contact area. The entire process of contact printing was executed for about 60 s. For a heterogeneous surface, the OTS-inked stamp containing patterns was used for a total contact time of 60 s. Each sample was kept in a glass Petri dish at room temperature for 1 h. Then, the contact-printed samples were sonicated with toluene for 2 min, removed, dried under a stream of N_2, and characterized within 4 h. The other heterogeneous surface was generated by using FTS/DTS monolayers prepared with the predeposited volume ratios of 50/50 and 0.1/99.9. Each mixed monolayer was masked with thin strips of Scotch tape having a width of a few hundred microns or millimeters. They were placed about 1 mm apart and then treated with UV/O oxidization for 10 min. After UV/O treatment, the Scotch tapes were peeled off, and the surfaces were cleaned with a cotton swab wetted with acetone.

PS Thin Film Generation. The FTS/DTS- and OTS-modified surfaces had low surface energies, so direct spin coating of PS solution onto these surfaces was difficult. Therefore, the "float-off and pick-up" method[15] to place a thin film of PS onto each organosilane-modified surface was applied. A 2 wt % PS solution

(44) Ferguson, G. S.; Chaudhury, M. K.; Biebuyck, H. A.; Whitesides, G. M. *Macromolecules* **1993**, *26*, 5870.

(in HPLC toluene) was passed through a microfilter (Acrodisc 13 mm syringe filter with 0.45 μm nylon membrane, Gelman) to remove any impurities. Then it was spin coated at 3000 rpm for 30 s using a spin coater (P-6000, Specialty Coating Systems) onto a 2.5 cm × 2.5 cm precleaned microscope glass slide. The PS thin film placed on the organosilane-treated silicon wafer was dried under ambient conditions inside a glass Petri dish for about 15 h. After drying, the samples were stored in a vacuum oven (~30 in. Hg) at 80 °C for 15 h to eliminate any residual water trapped at the PS film/organosilane-modified silicon wafer interface.

Sample Processing. *PS Thin Film Dewetting*. The PS thin films on the SAMs of organosilane were annealed at 160 °C using a hot plate under the ambient conditions. The proper annealing temperature and the film thickness of 800 Å were chosen by a simple combinatorial method.[45] At those conditions, dewetting velocity became measurable over the range of surface energy variation. An optical microscope (Infini Tube, Edmond Scientifics) equipped with a CCD video camera was used to follow the dewetting process from hole initiation to coalescence. Dewetting behaviors were videotaped, and the diameter (D) of the dewetting holes for selected images at various annealing times (t) was measured. The maximum distance of the inside rim was measured as the diameter. The very early stage (when the hole initiates) and the final stage (when the hole growth starts to level off or holes start to coalesce with each other) of dewetting were not considered in our measurements. The annealing was ceased immediately prior to the coalescence of holes. The dewetting velocity (V_D) was obtained from the slope of the linear relationship of D as a function of t. The correlation plots between the diameter (D) of dewetting holes and the surface energies (γ_S) at a particular annealing time were also generated. The dewetting hole information at a particular annealing time was obtained by removing the sample from the hot plate, quenching to room temperature, and measuring the diameter of holes throughout the dewetted area.

Sample Characterization. *Scanning Probe Microscopy*. The surfaces modified with organosilanes were first characterized with a SPM (Molecular Imaging Corp., MI 2000) to verify and analyze the formation of organosilane SAMs. Topographic and lateral force images were taken in contact mode using a 450 μm long cantilever having a spring constant of 0.2 nN/nm. Phase images were also taken with the noncontact mode to verify the phase separation of FTS/DTS mixed SAMs. A 125 μm long cantilever with a spring constant of 42 nN/nm and a frequency of 330 kHz was used for the noncontact mode scans. Various scan sizes, from 200 nm × 200 nm to 10 μm × 10 μm, were conducted.

Contact Angle. The modified silicon wafer was then examined with contact angle measurements via the sessile drop method. Contact angles were measured using deionized water ($\gamma_L^D = 22.0$ mJ/m^2, $\gamma_L^P = 50.2$ mJ/m^2, $\gamma_L = 72.2$ mJ/m^2) and methylene iodide ($\gamma_L^D = 48.5$ mJ/m^2, $\gamma_L^P = 2.3$ mJ/m^2, $\gamma_L = 50.8$ mJ/m^2) with a Rame-Hart contact angle goniometer, model 100-00. Four images of advancing (θ_A) and receding (θ_R) angles on two randomly chosen spots from each sample were taken using image-capturing equipment (Dazzle DVC, Dazzle media). The contact angles on both sides of the droplet were measured using the Scion Image. An average value (θ_{Avg}) of all the contact angles was used in calculating surface energy. Owens-Wendt geometric mean with the two-liquid method[2,25] was applied. The measurements were performed under ambient conditions (1 atm, 24 ± 2 °C).

Film Thickness Measurement. The thicknesses of polystyrene thin films were measured using an ellipsometer (model 439, Rudolph Instruments) with a helium−neon laser (λ = 6328 Å). The angle of incidence was 70° normal to the surface. The compensator was set at +45°. The refractive index of 1.592 was used for PS in calculating the film thickness. The accuracy of the film measured with this ellipsometer is ±2 Å.

Acknowledgment. We are grateful for financial support from the Start-Up Fund from the College of Engineering and the Department of Chemical Engineering at The University of Akron. We thank Mr. Joong-Hyun Chun for the valuable discussion on the chemistry of organosilanes. We also thank Dr. Teresa Cutright, Mr. Robert Newby, and Mr. Eugene J. Choi for proofreading our manuscript.

LA026489M

(45) Meredith, J. C.; Smith, A. P.; Tona, A.; Elgendy, H.; Karim, A.; Amis, E. *Polym. Mater. Sci. Eng.* **2001**, *84*, 1065.